2 was determined by tabular integration of the average observed heat capacities as a function of temperature in the anomaly, and the last term was determined by integrating the heat capacity equation above the anomaly over the temperature range of the tabular integration. The values for the enthalpy of transition calculated in this manner are listed in Table II and shown in Figure 1.

Values for heat capacity and enthalpy change above 298.15 K at even intervals of temperature for the phosphoric acids were calculated from the heat-capacity equations, their integrals with the proper integration constants, and the heats of transition listed in Table II. These values are listed in Table III. Enthalpy changes above 298.15 K also were calculated at the same temperatures as those reported by Wakefield et al. (*1*), and the values compared in Figure 2. The results are in good agreement except at 72.6% P_2O_5, a concentration in which the enthalpy of transition is quite pronounced, and above 350 K (77 °C), the temperature of the transition. This discrepancy probably can be explained by the fact that only the energy released as the acid cools from the higher temperature to 298.15 K in a short period of time would be measured by the drop calorimeter. The slow release of energy as the acid converts from the high-temperature form to the low-temperature form, which takes several hours, would not be detected.

Values of heat capacity of the phosphoric acid calculated from the heat-capacity equations were plotted against concentration at each 10-degree interval of temperature, and smooth curves were drawn through the points. Values of heat capacity at each 10-degree interval of temperature for phosphoric acids at even intervals of concentration then were read from the curves. Values of the enthalpy of transition at even intervals of concentration were read from Figure 1. Equations were fitted to these values, and the heat capacities and enthalpy changes above 298.15 K were determined as described above and are listed in Tables IV and V, respectively. The temperatures were converted to Celsius to make the report compatible with the previous one (*1*).

Corrections for converting C_s to C_p, the heat capacity at constant pressure, based on vapor pressures and enthalpies of vaporization taken from the literature (*3*) and the assumption that the liquids occupied 75% of the encapsulated volumes were less than 0.001 cal deg^{-1} g^{-1} over most of the temperature ranges but did increase to 0.002 cal deg^{-1} g^{-1} when the liquids were near their boiling points. These corrections, approximately the same magnitude as the differences between the observed and calculated heat capacities, were considered to be within the precision of the measurements.

Literature Cited

(1) Wakefield, Z. T.; Luff, B. B.; Reed, R. B. *J. Chem. Eng. Data* **1972**, *17*, 420-3.
(2) Ginnings, D. C.; Furukawa, G. T. *J. Am. Chem. Soc.* **1953**, *75*, 522-7.
(3) Brown, E. H.; Whitt, C. D. *Ind. Eng. Chem.* **1952**, *44*, 615-8.

Received for review June 2, 1980. Accepted October 27, 1980.

Solubility of Acetone and Isopropyl Ether in Compressed Nitrogen, Methane, and Carbon Dioxide

Paul J. Hicks, Jr., and John M. Prausnitz*
Chemical Engineering Department, University of California, Berkeley, California 94720

Vapor-phase solubilities are reported for acetone and isopropyl ether in compressed nitrogen, methane, and carbon dioxide, in the range −50 to 50 °C and 17–63 bar. The experimental solubilities are reduced to obtain second virial cross-coefficients. Experimental cross-coefficients are compared to those calculated by using the square-well potential or the Hayden–O'Connell correlation.

There is little fundamental information concerning the interaction between a small nonpolar molecule (*2*) and a large polar molecule (*1*). To obtain such information, it is useful to measure the second virial cross-coefficient B_{12} which is directly related to the intermolecular potential Γ_{12}. This work reports experimental measurements which yield B_{12} for a number of binary polar–nonpolar mixtures. The experimental data obtained are the solubilities of acetone and isopropyl ether in compressed nitrogen, methane, and carbon dioxide.

These measurements are also of interest in chemical engineering because they provide the fundamental information needed to calculate solvent losses in an absorption process operating at advanced pressure.

This work is similar to that of Lazalde et al. (*1*), who studied the solubility of methanol in compressed gases.

Experimental Section

The experimental apparatus is similar to that used by Lazalde (*1*). There are some minor modifications made primarily to facilitate changing pressures in the apparatus. A schematic of the flow apparatus is shown in Figure 1.

A light (gaseous) component is equilibrated with a heavy (liquid) component at a given temperature and pressure. The gas phase is sampled and analyzed.

The light component is fed from a gas cylinder through a pressure regulator and a precooling/preheating coil to the two equilibrium cells arranged in series. The gas enters the bottom of each equilibrium cell, containing the liquid being studied, through a stainless-steel sparger whose average pore size is 5 μm. The slowly flowing gas is saturated with the liquid as it bubbles through the liquid. Two cells in series are used to ensure that the exiting gas is in equilibrium with the liquid. The top of each cell is packed with glass wool to remove any possible entrainment of the liquid in the gas. The gas exits the second cell through a section of tubing heated to prevent condensation of the heavy component. In this section the gas is expanded to atmospheric pressure. The volumetric flow rate is always less than 0.3 cm^3/s where the measured solubility is independent of the flow rate.

The constant-temperature bath containing the equilibrium cells is controlled by a Halikainen (Shell Development) thermotrol to ±0.05 °C or better except at −50 °C where it is controlled to ±0.15 °C or better. At low temperatures, the bath fluid is 95% ethanol; at high temperatures, it is water. Temperatures above −10 °C are measured with a set of liquid-in-glass calorimetric thermometers with an accuracy of ±0.1 °C. Temperatures between −10 and −25 °C are measured with a

0021-9568/81/1726-0074$01.00/0

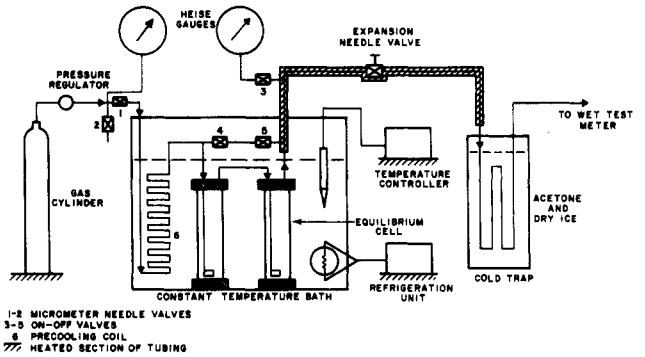

Figure 1. Schematic diagram of solubility apparatus.

liquid-in-glass precision thermometer tested by comparison with standards certified by the National Bureau of Standards with an accuracy of ±0.1 °C. Temperatures below −25 °C are measured with a Hewlett-Packard 2801A quartz thermometer with an accuracy of ±0.15 °C. The exit pressure is measured with a Heise pressure gauge with an accuracy of better than ±0.1 bar.

The exit gas passes through two condensers in series. They are at ∼−78 °C, except for the carbon dioxide systems where the temperature is ∼−40 °C. Each condenser contains a condensing liquid (e.g., toluene) and a small, known amount of internal standard (ethyl acetate); the condensing liquid is saturated with the gas being studied. Acetone (or ether) condenses into the condensing liquid while the light component (nitrogen, methane, or carbon dioxide) passes through to a wet test meter which measures the volume of the effluent gas with an accuracy of 1%. Upon completion of a run, the condensers are removed from the cold bath and mixed thoroughly. A 5-μL sample of the condensing liquid is analyzed by a Beckman Model GC-2A chromatograph with a digital integrator from Spectra-Physics, Inc. The column is 183 cm long and packed with Porapak Q supplied by Waters Associates. The amount of heavy component condensed is determined from the ratio of the area of the condensed liquid to that of the standard component. Calibration curves are made for this purpose; reproducibility is ∼1%.

Since the retention time in the chromatograph is long for toluene, it is sometimes preferable to use a different condensing liquid. For the experiments with ether (with nitrogen and methane), acetone is used instead of toluene.

Materials

Methane and carbon dioxide, obtained from Matheson, Inc., had specified minimum purities of 99.97 and 99.99%, respectively. Nitrogen was obtained from Liquid Carbonic Co. with a specified minimum purity of 99.996%. Acetone and isopropyl ether were obtained from Aldrich Chemical Co., Inc. Acetone was spectrophotometric grade with a specified minimum purity of 99+%. Isopropyl ether had a specified minimum purity of 99% and was distilled in a 13-tray Oldershaw column at high reflux. The top and the bottom 15% were discarded. It was necessary to distill the ether because the chromatograph showed impurities. Upon distillation these impurities were no longer detectable.

Results

Tables I and II show the solubilities of acetone and isopropyl ether in compressed nitrogen, methane, and carbon dioxide.

Thermodynamic Analysis

For the conditions encountered here, the compressed gas phase is well represented by the pressure-explicit virial equation truncated after the second term

$$z = Pv/(RT) = 1 + BP/(RT) \qquad (1)$$

Table I. Solubility of Acetone in Compressed Nitrogen, Methane, and Carbon Dioxide

gas	temp, °C	total press, bar	mole fraction acetone, $10^4 y_1$
nitrogen	35	55.0	135
	10	40.4	58.2
	10	55.2	50.9
	10	61.1	48.7
	−15	40.5	17.3
	−15	62.8	15.3
	−40	24.7	4.60
	−40	40.8	3.85
	−40	62.4	4.01
	−50	24.9	2.31
	−50	41.2	2.04
	−50	62.6	2.03
methane	50	31.0	356
	50	61.6	220
	0	31.3	50.5
	0	60.4	42.7
	−25	30.8	13.0
	−25	60.6	14.6
	−50	31.1	2.95
	−50	60.5	4.81
carbon dioxide	10	21.1	94.8
	−13	16.6	35.6

Table II. Solubility of Isopropyl Ether in Compressed Nitrogen, Methane, and Carbon Dioxide

gas	temp, °C	total press, bar	mole fraction isopropyl ether $10^4 y_1$
nitrogen	50	28.4	237
	50	55.6	154
	0	29.2	33.0
	0	55.5	28.3
	−25	30.3	8.33
	−25	56.2	7.89
	−50	30.3	1.47
	−50	56.6	1.75
methane	50	31.0	268
	50	58.0	198
	0	29.0	43.4
	0	58.1	37.4
	−25	29.0	12.1
	−25	57.0	16.8
	−25	58.1	18.4
	−50	29.5	2.27
	−50	58.0	7.13
carbon dioxide	50	26.4	272
	50	43.7	180
	25	26.5	120
	0	20.14	39.6
	−15	16.6	17.2

where P is absolute pressure, T is absolute temperature, v is the molar volume, R is the gas constant, and B is the second virial coefficient. One advantage of using this equation is that, in addition to pure-component parameters, only binary parameters (second virial cross-coefficients) are needed to describe multicomponent systems. Another advantage is that the composition dependence of the second virial coefficient of the mixture, B_M, can be derived from statistical mechanics:

$$B_M = \sum_i \sum_j y_i y_j B_{ij} \qquad (2)$$

where y_i and y_j are the gas-phase mole fractions of components i and j, respectively, and B_{ij} is the second virial coefficient describing the interaction between one molecule i and one molecule j. The second virial cross-coefficient, B_{12}, is determined as a function of temperature from the solubility data given in Tables I and II.

To determine B_{12}, it is necessary to solve the two equations of equilibrium:

$$f_1^V = f_1^L \qquad (3a)$$

$$f_2^V = f_2^L \quad (3b)$$

where f_1^V and f_1^L are the fugacities of component 1 (heavy component) in the vapor and liquid phases, respectively; subscript 2 refers to the light component. Fugacities in the vapor phase can be written as

$$f_1^V = y_1\phi P \quad (4a)$$

$$f_2^V = y_2\phi_2 P \quad (4b)$$

where ϕ is the fugacity coefficient. The fugacity of component 1 in the liquid phase can be written as

$$f_1^L = P_1^s\phi_1^s(1 - x_2)\gamma_1 \exp\{v_1^L(P - P_1^s)/(RT)\} \quad (5)$$

where v^L is the molar liquid volume, P^s is the saturated vapor pressure, ϕ^s is the saturated fugacity coefficient, and γ is the activity coefficient. Combining eq 3a, 4a, and 5 yields eq 6.

$$\phi_1 = \frac{\gamma_1(1 - x_2)P_1^s\phi_1^s \exp\left\{\dfrac{v_1^L(P - P_1^s)}{RT}\right\}}{y_1 P} \quad (6)$$

In eq 6, the gas-phase mole fraction, pressure, and temperature are measured experimentally, and the molar liquid volume and vapor pressure are taken or estimated from the literature (*2–6*). The saturated fugacity coefficient is taken to be unity since the liquid vapor pressures are small at the temperatures studied.

The liquid-phase mole fraction x_2 is related to f_2^L through the Krichevsky–Ilinskaya equation

$$\ln \frac{f_2^L}{x_2} = \ln H_{2,1}^{(P_1^s)} + \frac{A}{RT}(x_2^2 - 2x_2) + \frac{\bar{v}_2^\infty(P - P_1^s)}{RT} \quad (7)$$

where $H_{2,1}^{(P_1^s)}$ is Henry's constant at the given temperature and at the saturated vapor pressure, A is the Margules constant, and $\bar{v}^\infty$ is the partial molar volume at infinite dilution. Henry's constants for the acetone system are obtained from the literature (*7*); for the isopropyl ether systems they are obtained from correlations (*8–10*). The partial molar volumes at infinite dilution are determined from the literature (*2*) and from correlations (*9*).

The activity coefficient in eq 6 is estimated from the two-suffix Margules equation

$$\ln \gamma_1 = \frac{A}{RT}x_2^2 \quad (8)$$

Fortunately, the desired quantity (B_{12}) is not sensitive to A, and therefore a rough approximation is satisfactory. Here, Margules constants are estimated from Henry's constant, through the activity coefficient at infinite dilution:

$$\gamma_2^\infty = H_{2,1}/f_2^L(\text{pure}) \quad (9)$$

$$A = RT \ln \gamma_2^\infty \quad (10)$$

where the fugacity of pure "liquid" 2 at system temperature is calculated from a generalized correlation (*9*). Table III shows saturation pressures and molar volumes for the two liquids used here. Table IV shows Henry's constants, Margules constants, and partial molar volumes.

The fugacity coefficients are related to the pressure-explicit virial equation by eq 11a and 11b.

$$\ln \phi_1 = \{2(y_1B_{11} + y_2B_{12}) - B_M\}P/(RT) \quad (11a)$$

$$\ln \phi_2 = \{2(y_2B_{22} + y_1B_{12}) - B_M\}P/(RT) \quad (11b)$$

Equations 2–11 yield the second virial cross-coefficient, B_{12}. The calculation of B_{12} is sensitive to the experimental value of y_1. It is generally not sensitive to A, but it may be sensitive to $H_{2,1}$, as discussed later, if $H_{2,1}$ is small.

Table III. Vapor Pressures and Molar Volumes for Acetone and Isopropyl Ether

compd	T, °C	P_1^s,[a] bar	ν_1^L,[b] cm³/mol
acetone	50	0.8196	76.8
	40	0.5661	75.7
	35	0.4656	75.1
	25	0.3078	74.1
	10	0.1552	72.5
	0	0.09351	71.5
	−13	0.04514	70.2
	−15	0.04005	70.1
	−25	0.0212	69.1
	−40	0.0069	67.8
	−50	0.00313	67.0
isopropyl ether	50	0.5432	147.4
	25	0.1996	142.2
	0	0.0576	137.4
	−15	0.02359	134.6
	−25	0.01223	132.8
	−50	(0.00173)	128.6

[a] Values for P_1^s are experimental data or are estimated from experimental data (*2, 4–6*); the estimated datum is indicated by parentheses. [b] Values for ν_1^L are experimental data for acetone (*3*) and experimental data and estimates from correlations for isopropyl ether (*2, 15*).

Table IV. Henry's Constants, Margules Constants, and Partial Molar Volumes at Infinite Dilution[a]

binary	T, °C	$H_{2,1}$, bar	A, cm³ bar/mol	$\bar{\nu}_2^\infty$, cm³/mol
nitrogen-acetone	35	1750	51 300	55
	10	1950	50 300	54
	−15	2170	49 300	52
	−40	2380	48 800	51
	−50	2460	48 700	50
methane-acetone	50	583	26 500	56
	0	511	27 200	54
	−25	456	28 600	52
	−50	386	34 800	51
carbon dioxide-acetone	40	70.1	2 160–5 220	48
	25	51.5	875–3 600	47
	10	37.1	918	46
	−13	20.2	−642	45
nitrogen-isopropyl ether	50	(562)	23 000	57
	0	(628)	23 000	52
	−25	(675)	24 000	50
	−50	(660)	25 000	48
methane-isopropyl ether	50	(225)	0	60
	0	(173)	2 630	56
	−25	(150)	5 670	54
	−50	(106)	12 000	52
carbon dioxide-isopropyl ether	50	(101)	10 700	60
	25	(69.5)	9 730	58
	0	(32.0)	721	56
	−15	(20.3)	237	54

[a] Values for A are calculated as indicated by eq 9 and 10. Some values for $H_{2,1}$ are experimental (*7*), others are estimated (*10*); the estimated values are indicated by parentheses. Values for $\bar{\nu}_2^\infty$ are estimated (*2, 9*).

Second Virial Cross-Coefficients

Pure-component virial coefficients for nitrogen, methane, and carbon dioxide are taken from the literature (*1, 11*). Virial coefficients for acetone and isopropyl ether cannot be fit to the square-well potential with realistic parameters; the correlation of Tsonopoulos (*12*) is used here to estimate second virial coefficients for these fluids. Table V and Figures 2 and 3 show results for B_{12}.

The virial coefficients are related to a potential function which relates the intermolecular forces to a size parameter, σ, and

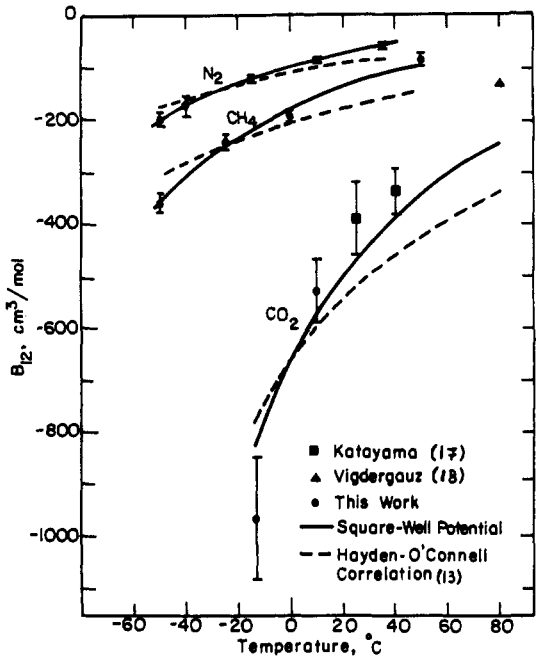

Figure 2. Second virial cross-coefficient for binary mixtures of acetone with nitrogen, methane, and carbon dioxide.

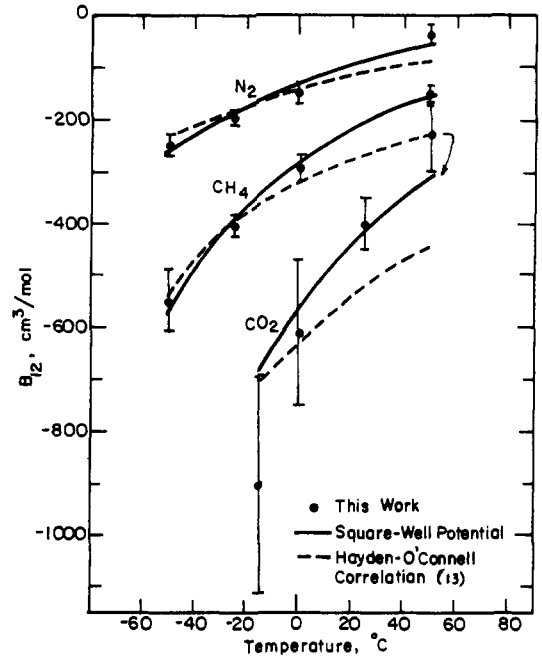

Figure 3. Second virial cross-coefficient for binary mixtures of isopropyl ether with nitrogen, methane, and carbon dioxide.

Table V. Second Virial Cross-Coefficients

binary	T, °C	B_{12}, cm³/mol
nitrogen-acetone	35.0	−58 ± 7
	10.0	−85 ± 7
	−15.0	−119 ± 7
	−40.0	−174 ± 19
	−50.1	−199 ± 13
methane-acetone	50.0	−84 ± 12
	0.0	−191 ± 13
	−25.0	−242 ± 15
	−50.0	−360 ± 17
carbon dioxide-acetone	10.0	−531 ± 60
	−13.0	−966 ± 120
nitrogen-isopropyl ether	50.0	−38 ± 20
	0.0	−149 ± 20
	−25.0	−195 ± 14
	−50.0	−248 ± 20
methane-isopropyl ether	50.0	−147 ± 12
	0.0	−293 ± 26
	−25.0	−405 ± 20
	−50.0	−550 ± 60
carbon dioxide-isopropyl ether	50.0	−223 ± 70
	25.0	−402 ± 50
	0.0	−610 ± 140
	−15.0	−903 ± 210

an energy parameter, ϵ (*9*). This relation enables virial coefficients to be interpolated and extrapolated with respect to temperature. As shown by Lazalde (*1*), the square-well potential appears to be suitable for describing interactions between small nonpolar molecules and somewhat larger polar molecules.

Square-Well Potential

The square-well potential, Γ, shown in Figure 4, is directly related to the second virial coefficient:

$$B_{ij} = \tfrac{2}{3}\pi N_a \sigma_{ij}^3 \left\{1 - (\mathbf{R}^3 - 1)\left(\exp\left(\frac{\epsilon_{ij}}{kT}\right) - 1\right)\right\} \quad (12)$$

where N_a is Avogadro's number and k is Boltzmann's constant. For pure nitrogen, methane, and carbon dioxide (B_{ii} or B_{jj}), pure-component parameters σ, ϵ, and **R** are required. Parameters for nitrogen, methane, and carbon dioxide are taken from Lazalde (*1*).

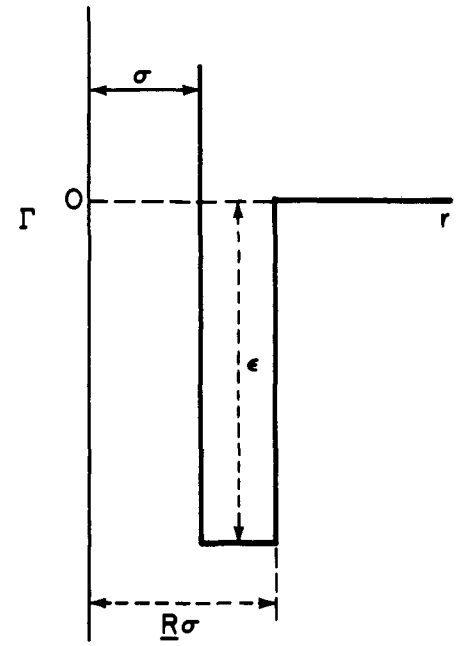

σ = collision diameter
ϵ = well depth
(R-1) = ratio of well width to σ

Figure 4. Square-well potential Γ.

For acetone and isopropyl ether, size parameter, σ, is estimated from Figure 5, which shows the cube root of the critical volume vs. experimental square-well values for σ. The "best" straight line from the origin is drawn through the experimental points.

To calculate the cross-coefficient, B_{ij}, we first investigated these mixing rules for σ_{ij} and ϵ_{ij}:

$$\sigma_{ij} = \tfrac{1}{2}(\sigma_{ii} + \sigma_{jj}) \quad (13)$$

$$\epsilon_{ij} = (\epsilon_{ii}\epsilon_{jj})^{1/2} \quad (14)$$

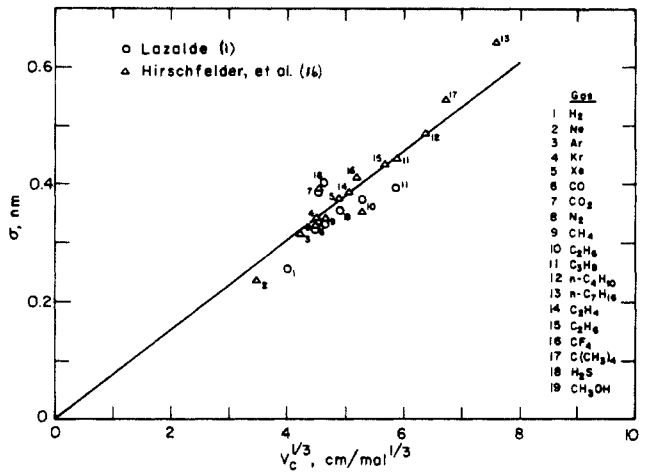

Figure 5. Estimation of σ for square-well potential.

Table VI. Parameters for Square-Well Potential

compd	σ, nm	ϵ/k, K
acetone	0.44	979
isopropyl ether	0.57	967
binary		c, K
nitrogen–acetone		55
methane–acetone		55
carbon dioxide–acetone		150
nitrogen–isopropyl ether		40
methane–isopropyl ether		57
carbon dioxide–isopropyl ether		73

For each binary, $\mathbf{R}_{ij}$ and ϵ_{ij} are calculated from the experimental data and from eq 12 by using a nonlinear regression which minimizes the sum of the squared errors. For the polar component, ϵ is then calculated from eq 14. One $\mathbf{R}_{ij}$ is desired for all binary systems. However, the best $\mathbf{R}_{ij}$, based on the criteria of minimizing the sum of the squared errors, is $\sim$1.13 for the binary systems containing nitrogen or methane, 1.02 for the carbon dioxide–isopropyl ether system, and 1.01 for the carbon dioxide–acetone system. These values, especially for the carbon dioxide–containing systems, are unreasonably small and lead to very large values of ϵ for acetone and isopropyl ether.

Because of polarity, the theory of intermolecular forces suggests that there should be a temperature-dependent correction to eq 14. Following Lazalde (*1*) and setting $\mathbf{R}$ = 1.2, we assume

$$\epsilon_{ij} = (\epsilon_{ii}\epsilon_{jj})^{1/2}(1 + c/T) \qquad (15)$$

where c is a positive constant accounting for orientational effects. Table VI gives experimental values for σ, ϵ, and c.

As expected from Lazalde's experience, eq 15 gives better results; the nitrogen- and methane-containing binary systems can be fitted well. However, the carbon dioxide-containing systems are not described adequately. The square-well potential is unable to reproduce the very strong temperature dependence of B_{12} shown in Figures 2 and 3.

Hayden–O'Oconnell Correlation

The Hayden–O'Connell correlation (*13*) is an extension of the corresponding-states correlation presented earlier by O'Connell and Prausnitz (*14*). Hayden and O'Connell take into account association between molecules with an association parameter, η.

As shown in Figures 2 and 3, the correlation of Hayden and O'Connell is unable to represent B_{12} data for the carbon dioxide–acetone and carbon dioxide–isopropyl ether systems; calculated results are no better than those obtained from the square-well potential. In addition, the correlation is also poor for the nitrogen- and methane-containing systems. The one adjustable binary parameter appears to be inadequate to fit both the magnitudes and the slopes of the curves. Best values for η are given in Table VII.

Table VII. Association Parameters for Hayden–O'Connell Correlation

binary	η
nitrogen–acetone	0.156
methane–acetone	0.168
carbon dioxide–acetone	0.559
nitrogen–isopropyl ether	~0
methane–isopropyl ether	0.040
carbon dioxide–isopropyl ether	0.339

Error Analysis

There is necessarily some experimental error in the measurement of temperature, pressure, and gas-phase mole fraction. There is also some uncertainty in properties taken from the literature and in those estimated from correlations. The uncertainty introduced by B_{12} by experimental errors in P, T, B_{22}, $\bar{v}_2^{\infty}$, and v_1^{L} are always small compared to those from other sources. The largest uncertainty in B_{12} is due to errors in P_1^s, B_{11}, y_1, or $H_{2,1}$. Errors in y_1 and B_{11} are the most significant for the nitrogen- and methane-containing binaries at higher temperatures. Errors in P_1^s (and sometimes y_1) are the most significant for these systems at the lower temperatures.

However, for the carbon dioxide-containing binaries, errors in $H_{2,1}$ are generally the most important sources of uncertainty in B_{12}. As indicated in Figures 2 and 3, the uncertainties in B_{12} are large; they are due almost entirely to errors in the Henry's constant, especially at the lower temperatures where $H_{2,1}$ is small. For the carbon dioxide–acetone system, there are a few literature values for Henry's constant, but these are scattered and probably of low accuracy. For the carbon dioxide–isopropyl ether system, there are no experimental values, and the accuracy of the correlation is uncertain. As reported here, estimated errors for Henry's constants are based on how well the correlation predicts Henry's constants for the carbon dioxide–ethyl ether system, since experimental results for that system are available for comparison.

Discussion

The square-well potential is suitable for representing second virial coefficient data for the nitrogen- and methane-containing binaries. However, for the carbon dioxide-containing systems the square-well potential appears to be inadequate. The Hayden–O'Connell correlation is also not satisfactory.

The inability of the two models to fit the experimental data is probably due to one (or both) of two reasons. First, the models may not be able to describe the carbon dioxide–acetone and carbon dioxide–isopropyl ether interactions because of some strong specific interaction between the two dissimilar molecules. Second, the calculated values for B_{12} may be in error. High errors in B_{12} are introduced by uncertainties in Henry's constants.

For engineering calculations, we suggest that the cross-coefficients calculated by using the square-well potential (Figures 6 and 7) are likely to provide better estimates than the experimental values which are calculated by using questionable data for Henry's constants. This suggestion is plausible considering that the B_{12} values calculated from the square-well potential are essentially within the error bars at each experimental point. Error bars represent uncertainty due to all causes, especially due to estimated inaccuracy of Henry's

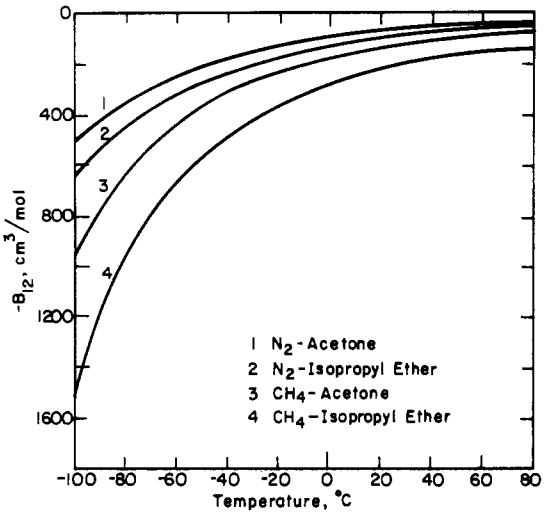

Figure 6. Second virial cross-coefficients calculated by using the square-well potential.

Table VIII. Henry's Constants From B_{12} as Calculated from the Square-Well Potential

binary	T, °C	$H_{2,1}$, bar
carbon dioxide–acetone	40.0	51.1
	25.0	41.9
	10.0	30.9
	−13.0	27.5
carbon dioxide–isopropyl ether	50.0	57.0
	25.0	66.9
	0.0	37.9
	−15.0	32.4

constants. If more reliable Henry's constants can be obtained, the solubility data presented here may be used for more accurate calculation of B_{12}.

Table VIII gives those Henry's constants needed to obtain the B_{12} values predicted by the square-well potential model. The Henry's constants shown for the carbon dioxide–acetone system are reasonable. Those for the carbon dioxide–isopropyl ether system are of the right order of magnitude but are not reliable because Henry's constant predicted at 25 °C is larger than that at 50 °C. A comparison of these Henry's constants with those in Table IV gives a measure of the sensitivity of B_{12} to the Henry's constant. Errors in calculated gas-phase solubilities are not as large as the error estimates in B_{12} seem to indicate provided the same Henry's constants are used as those used in the calculation of B_{12}. Figures 6 and 7 show calculated second virial cross-coefficients for the square-well potential. For engineering purposes, these are probably the most reliable values now available.

Conclusions

Experimentally measured gas-phase solubilities of acetone and isopropyl ether in compressed nitrogen, methane, and carbon dioxide are reported for the temperature range −50 to 50 °C and the pressure range 17–63 bar. The accuracy of these solubilities is ~3%.

Second virial cross-coefficients for each binary system are estimated and fitted to the potential energy function. The fits are good for the systems containing nitrogen or methane. There is less certainty in the results for the carbon dioxide-containing binaries. Nevertheless, the second virial cross-coefficients reported here may be useful for engineering calculations to determine solvent losses in high-pressure absorption operations using acetone or isopropyl ether as solvents.

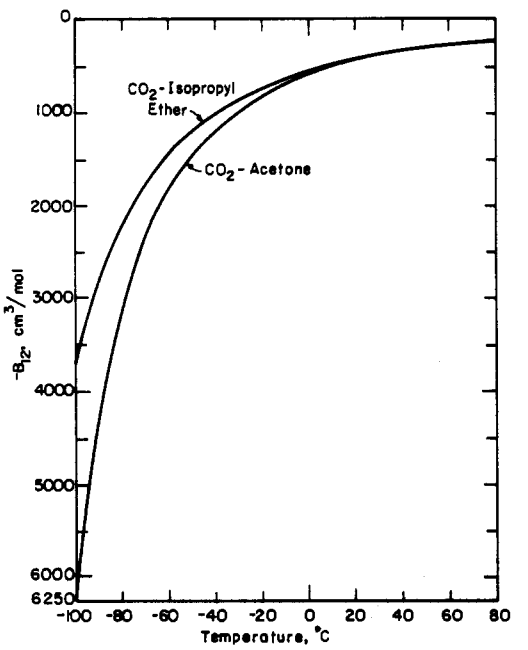

Figure 7. Second virial cross-coefficients calculated by using the square-well potential.

Glossary

A	Margules constant, cm^3 bar/mol
B	second virial coefficient, cm^3/mol
c	constant, eq 15, K
f	fugacity, bar
$H_{2,1}$	Henry's constant for solute 2 in solvent 1, bar
k	Boltzmann constant
P	total pressure, bar
P^s	vapor pressure, bar
R	gas constant
R	reduced well width for square-well potential
T	absolute temperature, K
v	molar volume, cm^3/mol
$\bar{v}$	partial molar volume, cm^3/mol
x	liquid-phase mole fraction
y	gas-phase mole fraction
z	compressibility factor

Greek Letters

Γ	potential function, J
γ	activity coefficient
ϵ	energy parameter, J
η	association parameter, Hayden-O'Connell correlation
σ	size parameter, nm
ϕ	fugacity coefficient

Subscripts

i,j	components
1	heavy component
2	light component
M	mixture

Superscripts

L	liquid phase
s	saturation
V	vapor phase
∞	infinite dilution

Literature Cited

(1) Lazalde, H.; Breedveld, G.; Prausnitz, J. M. *AIChE J.* **1980**, *26*, 462.
(2) Reid, R. C.; Prausnitz, J. M.; Sherwood, T. K. "The Properties of Gases and Liquids"; McGraw-Hill: New York, 1977.
(3) Timmermans, J. "Physico-Chemical Constants of Pure Organic Compounds"; Elsevier: New York, 1950.

(4) Boublik, T.; Fried, V.; Hala, E. H. "The Vapor Pressures of Pure Substance"; Elsevier: Amsterdam, 1973.
(5) Felsing, W. A.; Durban, S. A. *J. Am. Chem. Soc.* **1926**, *48*, 2885.
(6) Washburn, E. W., Ed. "International Critical Tables of Numerical Data, Physics, Chemistry and Technology"; McGraw-Hill: New York, 1928; Vol. 3.
(7) "Landolt-Bornstein Zahlenwerte und Funktionen 6. Auflage IV. Band Tecknik, 4. Teil Wärmetechnik Bestandteil cl, Absorption in Flüssigkeiten mit niedrigem Dampfdruck"; Springer-Verlag: Berlin, 1976.
(8) Lyckman, E. W.; Eckert, C. A.; Prausnitz, J. M. *Chem. Eng. Sci.* **1965**, *20*, 703.
(9) Prausnitz, J. M. "Molecular Thermodynamics of Fluid-Phase Equilibria"; Prentice-Hall: Englewood Cliffs, NJ, 1969.
(10) Rivas, O. Ph.D dissertation, University of California, Berkeley, CA, 1978.
(11) Dymond, J. H.; Smith, E. B. "The Virial Coefficients of Gases"; Clarendon Press: Oxford, 1969.
(12) Tsonopoulos, C. *AIChE J.* **1974**, *20*, 263.
(13) Hayden, J. G.; O'Connell, J. P. *Ind. Eng. Chem. Process Des. Dev.* **1975**, *14*, 209.
(14) O'Connell, J. P.; Prausnitz, J. M. *Ind. Eng. Chem. Process Des. Dev.* **1967**, *6*, 245.
(15) Fife, H. R.; Reid, E. W. *Ind. Eng. Chem.* **1930**, *22*, 513.
(16) Hirschfelder, J. O.; Curtiss, C. F.; Bird, R. B. "Molecular Theory of Gases and Liquids"; Wiley: New York, 1954.
(17) Katayama, T. *J. Chem. Eng. Jpn.* **1975**, *8*, 89.
(18) Vigdergauz, M.; Semkin, V. *J. Chromatogr.* **1971**, *58*, 95.

Received for review May 20, 1980. Accepted October 17, 1980. Acknowledgement is made to the donors of the Petroleum Research Fund, administered by the American Chemical Society, for support of this research. This research was also supported by grants from the National Science Foundation and the Deutsche Forschungsgemeinschaft.

Pressure Effects on Conductivity and Ionic Association of Some Monovalent Salts in Aprotic Dipolar Solvents

Paul G. Giugia, Jae H. Byon, and Charles A. Eckert*

Department of Chemical Engineering, University of Illinois, Urbana, Illinois 61801

The conductance of LiI, LiBr, and NaI in acetonitrile and of tetra-*n*-butylammonium iodide and tetra-*n*-butylammonium bromide in acetone and in 4-methyl-2-pentanone were measured as a function of pressure. Data are reported at 25 °C over a concentration range of 0.0001–0.03 M and at pressures up to 2–3 kbar. Analysis of these data using Justice's modification of the Fuoss–Onsager equation yields values of the limiting conductance and the association constants as a function of pressure. Both the limiting conductance values and the association constants decrease with increasing pressure, and from the latter values of the volume change on association are calculated.

Introduction

High pressure is an extremely powerful tool for the study of reaction mechanisms and kinetic solvent effects, by careful measurement of variations in the volume of activation (*1*, *2*). In order to make such studies on ionic reactions in dipolar aprotic solvents, the degree of dissociation as a function of pressure must be well-known, as most often only the dissociated ion is kinetically active (*3*, *4*). Conductance measurements yield both the association constant as well as information about the relative solvating ability of solvents for various ions. High-pressure determinations yield, as well as the association constant, the limiting conductance as a function of pressure, and the volume change for ion-pair formation.

The conductance of NaI, LiI, and LiBr was measured in acetonitrile. The conductance of tetra-*n*-butylammonium iodide (Bu_4NI) and tetra-*n*-butylammonium bromide (Bu_4NBr) was measured in acetone and in 4-methyl-2-pentanone. These combinations of salts and solvents were chosen for use in conjunction with a kinetic study of a halide-exchange reaction under pressure (*5*).

Experimental Section

A diagram of the high-pressure conductance cells that were used in this study is shown in Figure 1. The main body of each cell was Teflon, to resist pressure cycling, but the platinum plates were firmly supported in glass to minimize the variation in cell constant with pressure. The cells were attached to a mercury reservoir, and each contained ~40 mL of electrolyte and 20 mL of mercury. Two cells were used with cell constants of ~0.05 and 0.5. These cell constants were measured as a function of pressure by using the data of Fisher (*6*) and Fuoss (*7*) for KCl in water. The variation in cell constant to 3 kbar was much less than 1%.

The pressure system was essentially similar to that used in a previous study of this type (*8*); measured pressures are accurate to ±2 bar and temperatures to ±0.01 °C.

The chemicals used in this study were purified according to the procedure suggested by Perrin (*9*).

Lithium iodide from Mallinckrodt Chemical Works was recrystallized from acetone. The filtered lithium iodide solution was evaporated at room temperature under vacuum. The residual hydrated crystal was dried at 60 °C under vacuum for 2 h and then at 120 °C under high vacuum by using the Abderhalden drying apparatus.

Lithium bromide from Fisher Scientific Co. was recrystallized several times from water and then dried under high vacuum at room temperature, followed by drying at 100 °C.

Sodium iodide from Mallinckrodt Chemicals Works (purity 99.5%) was recrystallized from ethanol and dried for 12 h under vacuum at 70 °C.

$(Bu)_4NI$ was obtained from Eastman Kodak Co. and was dried for 24 h under strong vacuum at room temperature in the presence of P_2O_5. Solutions of $(Bu)_4NI$ were prepared by weight and checked by titration with $AgNO_3$ solutions. The determinations always agreed within 1%. $(Bu)_4NI$ solutions were shaken with starch solutions, and no color change due to I_2 was observed. Karl Fisher titrations showed no water.

$(Bu)_4NBr$ was obtained from Matheson Coleman and Bell. It was dried for 24 h under strong vacuum in the presence of P_2O_5. Solutions of $(Bu)_4NBr$ were prepared by titration with $AgNO_3$. Karl Fisher titrations showed no water.

Acetonitrile was Baker's analyzed reagent grade and was dried by shaking with Linde 4A molecular sieves and then stirred with calcium hydride until no further hydrogen was evolved. The acetonitrile was then fractionally distilled at a high reflex ratio.

0021-9568/81/1726-0080$01.00/0